Vol 18 No 8, August 2009
1674-1056/2009/18(08)/3271-08

Chinese Physics B

© 2009 Chin. Phys. Soc.
and IOP Publishing Ltd

A modified weighted probabilistic cellular automaton traffic flow model*

Zhuang Qian(庄 倩), Jia Bin(贾 斌)†, and Li Xin-Gang(李新刚)

School of Traffic and Transportation, Beijing Jiaotong University, Beijing 100044, *China*

(Received 31 December 2008; revised manuscript received 5 February 2009)

This paper modifies the weighted probabilistic cellular automaton model (Li X L, Kuang H, Song T, *et al* 2008 *Chin. Phys.* B **17** 2366) which considered a diversity of traffic behaviors under real traffic situations induced by various driving characters and habits. In the new model, the effects of the velocity at the last time step and drivers' desire for acceleration are taken into account. The fundamental diagram, spatial-temporal diagram, and the time series of one-minute data are analyzed. The results show that this model reproduces synchronized flow. Finally, it simulates the on-ramp system with the proposed model. Some characteristics including the phase diagram are studied.

Keywords: synchronized flow, probabilistic distribution function, on-ramp system, cellular automaton

PACC: 0520, 0550

1. Introduction

During the last few decades, lots of scientists in the field of physics and mathematics have devoted themselves to traffic flow modeling. A variety of traffic flow models are presented, including car-following models, cellular automaton models, continuum models, gas-kinetic models, etc.[1−4] As a class of microscopic traffic flow models, cellular automaton models have attracted much attention because of their unique advantages. Since Nagel and Schreckenberg proposed the famous NaSch model[5] to study highway traffic, a large number of cellular automaton models[6−13] have sprung up, such as the FI model,[14] and the VE model.[15] These cellular automaton models discuss the non-linear traffic phenomena by modeling traffic systems from different perspectives.

In real traffic circumstances, there exist various vehicle types and driving styles. Thus a driver mostly reacts differently from others even to the same traffic situation due to the diversity of vehicle performance and drivers' personality. Otherwise, noises or disturbances also affect driving behaviors. However, the NaSch model and its derivatively improved models cannot describe driving behaviors determined by both internal and external factors. Masahiro Kanai *et al*[16] proposed a stochastic cellular automaton model inspired by the optimal velocity model.[17−18] Considering the mechanism of vehicle acceleration from the macroscopic statistical viewpoint, Li *et al*[19] recently presented a weighted probabilistic cellular automaton model (WP model) by introducing a weighted random acceleration probability distribution function to synthetically describe the variety of traffic behaviors caused by drivers, vehicles, noises and external influences. However, the flow rate in Li's model is a little smaller than the real data. And in Li's model, it is possible that velocity abruptly changes greatly for no reason from time step t to $t+1$, which means velocity fluctuates sharply at contiguous time step. It is not consistent with real traffic.

In this paper, we improve the original WP model by considering the effect of velocity at the last time step. Because of the continuity of driving, a vehicle's velocity at time $t+1$ is not independent of that at time t. On the contrary, the former is obtained by accelerating or decelerating on the basis of the latter. Moreover, all drivers tend to drive at their desired velocities, which implies that acceleration is preferred rather than deceleration unless the gap is not allowed for safety. Thus in our modified WP model (MWP model), the deceleration of vehicles is restricted. In addition, in an on-ramp system, vehicles near the

*Project supported by the State Key Development Program for Basic Research of China (Grant No 2006CB705500), the National Natural Science Foundation of China (Grant Nos 70631001, 70501004 and 70701004), and Program for New Century Excellent Talents in University (Grant No CET-07-0057).

†Corresponding author. E-mail: bjia@bjtu.edu.cn

on-ramp often perform with more sensitiveness, complexity and uncertainty, which implies that the MWP model may present a better description of drivers' behaviors near the bottlenecks.

This paper is organized as follows. In Section 2, the MWP model is presented in detail. In Section 3, a single-lane system under the periodic boundary and an on-ramp system under open boundaries are simulated respectively, and the simulation results are discussed in detail. Finally, the conclusions are given in Section 4.

2. Model

In the CA model, time, space and velocity are all discrete. The road is composed of discrete sites (cell), and each cell is either occupied by one vehicle or is empty. The velocity of the vehicle can be one of the values belonging to $0 \to v_{\max}$, where $v_{\max}$ is the maximum velocity. It should be emphasized that considering the diversity of drivers and vehicles, we find that the maximum velocity only denotes the maximum value of expectations of speed and does not imply the maximum velocity of each vehicle. At time $t \to t+1$, the evolution rules of the WP model are given as follows.[19]

First of all, let M_i^t be a stochastic variable which denotes the number of cells that the vehicle i hops at time t. The m denotes a probable value of M_i^t. A probability distribution function $w_i^t(m)$ is introduced which gives the probability of the vehicle i hopping m sites ahead at time t. That is the probability of $M_i^t = m$.

The probability distribution function is defined as follows:

$$w_i^t(m) = \begin{cases} 1, & \Delta x_i = 0, \\ \dfrac{1}{\Delta x_i}\left(1 - \dfrac{\alpha}{\gamma^{m+1}}\right), & m = 0, 1, \cdots, \ \Delta x_i - 1; \ \Delta x_i \neq 0, \\ \dfrac{1}{\Delta x_i}\left(1 - \dfrac{\beta}{\gamma^{m}}\right), & m = \Delta x_i; \ \Delta x_i \neq 0, \end{cases} \tag{1}$$

where α, β and γ are undetermined parameters which should meet the requirements that $\alpha,\ \beta,\ \gamma \in Z^+$, $\alpha+\beta=\gamma$, $\gamma > 1$, and $\alpha > \beta$; x_i^t denotes the position of the vehicle i at time t, while x_{i+1}^t denotes the position of the vehicle $i+1$ at time t. The $\Delta x_i = x_{i+1}^t - x_i^t - 1$ denotes the number of empty cells in front of vehicle i, i.e. the gap. It should be noted that as a result of $m_{\max} = v_{\max}$ when $\Delta x_i > v_{\max}$, let $\Delta x_i = v_{\max}$ in order to guarantee that $m \leq m_{\max}$ and the probable value of m is $0, 1\ \cdots$, or Δx_i.

It shows the properties of $w_i^t(m)$ as follows:

(i) When Δx_i is given, drivers generally move as fast as possible. So $w_i^t(m)$ $(m = 0, 1, \cdots, \Delta x_i; v_{\max} \geq \Delta x_i > 0)$ increases monotonically with the increase of m at a given Δx_i which means $w_i^t(m)/w_i^t(m-1) > 1$. However, because of the restrictions of external influences (e.g. speed limit) and internal factors (e.g. vehicle performance), the ratio is close to 1 as m increases, that means $w_i^t(m)/w_i^t(m-1) \to 1\,(m \to \Delta x_i)$, which reflects that the acceleration effect is almost the same at larger gaps;

(ii) $\sum_{m=0}^{\Delta x_i^t} w_i^t(m) = 1$, and $w_i^t(m) = 1$, when $\Delta x_i = 0$, which means that $w_i^t(m)$ obeys the unitary condition.

At time $t \to t+1$, the parallel update rules of the model are as follows:

Step 1 Determination of the randomization parameter $w_i^t(m)$ based on Eq.(1) at a given Δx_i.

Step 2 Determination of the number of sites which a vehicle hops (i.e. the probability speed) according to the intention $w_i^t(m)$. According to Eq.(1), the set of probability density composes of the following $\Delta x_i + 1$ subsets:

$$\begin{aligned} &1) \quad \left[0, w_i^t(0)\right); \\ &2) \quad \left[w_i^t(0), w_i^t(0) + w_i^t(1)\right); \\ &\cdots; \\ &\Delta x_i) \quad \left[w_i^t(0) + \cdots + w_i^t(m-2), \right. \\ &\qquad \left. w_i^t(0) + \cdots + w_i^t(m-1)\right); \end{aligned}$$

$$\Delta x_i + 1) \quad [w_i^t(0) + \cdots + w_i^t(m-1), 1].$$

Step 3 During the computation, for certain Δx_i, the random number rand $(\cdot)$ is produced by computer, and rand $(\cdot) \in [0, 1]$. If rand $(\cdot)$ belongs to the j-th ($j = 1, 2, \cdots, \Delta x_i + 1$) one of the subsets in step 2, the number of sites which a vehicle hops is $m = j - 1$.

$$v_i^t = m, \tag{2}$$

where v_i^t denotes the velocity of vehicle i at time t.

Step 4 Update the new position of each vehicle

$$x_i^{t+1} = x_i^t + v_i^t, \tag{3}$$

where x_i^{t+1} denotes the position of vehicle i at time $t + 1$.

From updated rules of the WP model, we can see that the velocity may fluctuate sharply from time step t to $t + 1$. For example, the velocity is $v_{\max}$ at time t, but it may be 0 at time $t + 1$ without any reason. It does not accord with real traffic. So we improve step 3 of the updated rules of the WP model as follows.

Considering that deceleration of the vehicle changes in a certain range and the velocity at time $t + 1$ changes depending on the velocity at time t, we get the velocity range at time $t + 1$,

$$v_i^t \in \left[v_i^{t-1} - 1, \min\left(v_{\max}, \Delta x_i\right)\right], \; v_i^t \in Z^+. \tag{4}$$

If $v_i^{t-1} - 1 < 0$, the lower bound of the range equals 0; If $v_i^{t-1} - 1 > \Delta x_i$, let $v_i^t = \Delta x_i$. According to the property of the distribution function and $w_i^t(m)$, we can determine the probability range

$$\left[w_i^t(0) + \cdots + w_i^t\left(v_i^{t-1} - 2\right), 1\right], \tag{5}$$

which corresponds to the velocity range (4). A random number which is uniformly distributed in the range is produced. If the random number belongs to the j-th subset in step 2 of the updated rules of the WP model, we set $m = j - 1$. Other updated rules of our model are the same as those of the WP model.

3. Simulation results

The numerical simulations are performed on a single-lane road which is divided into a one-dimensional array of L sites, then the results are analyzed and discussed. In the simulation, each site corresponds to 7.5 m, each vehicle which holds the length of one site and one time step is 1 s. The parameters in the model are $v_{\max} = 5$, $L = 1000$. Furthermore, similar to the WP model, let $\alpha = 2$, $\beta = 1$, $\gamma = 3$. The first 10000 time-steps are put away in order to remove the transient effects, and then the data are recorded in successive 50000 time-steps.

3.1. Single lane system

In this subsection, the periodic boundary condition is adopted.

Figure 1 shows the fundamental diagram and plot of average velocity versus density of the MWP model and the WP model. It shows that the flow rate in the MWP model is higher than that in the WP model when the density is not large. The main reason is that the maximal deceleration of the vehicle in the MWP model is 1, while that in the WP model is unrestricted. So the velocity in the MWP model is higher than that in the WP model, which leads to the higher flow rate in the MWP model at the same density. In addition, it can be seen that there exists a critical density k_c. The velocity curve is concave when $k < k_c$, so the flow rate increases with the increase of density. The flow rate reaches its maximum level at $k = k_c$. When $k > k_c$, as the gap becomes smaller with the increase of density, the average velocity begins to decrease sharply. The velocity curve becomes convex and the flow rate starts to decrease as the density rises.

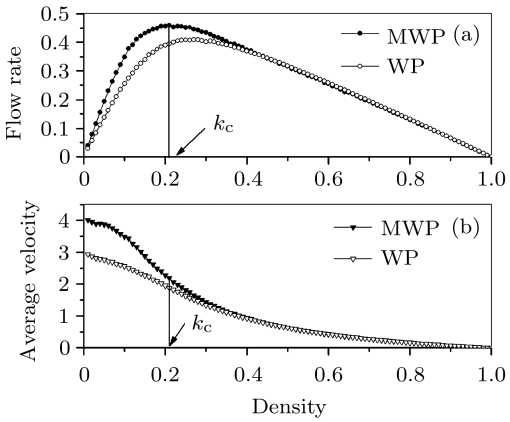


Fig.1. Fundamental diagram and average velocity diagram of the MWP model and the WP model.

Figure 2 shows the spatial-temporal diagram of the MWP model. When $k = 0.05$, every vehicle can be driven at the desired velocity (Fig.2(a)). When $k = 0.26$, the traffic flow is quite homogeneous and there is no spontaneous jam, which seems to exhibit spatiotemporal features of synchronized flow (Fig.2(b)).

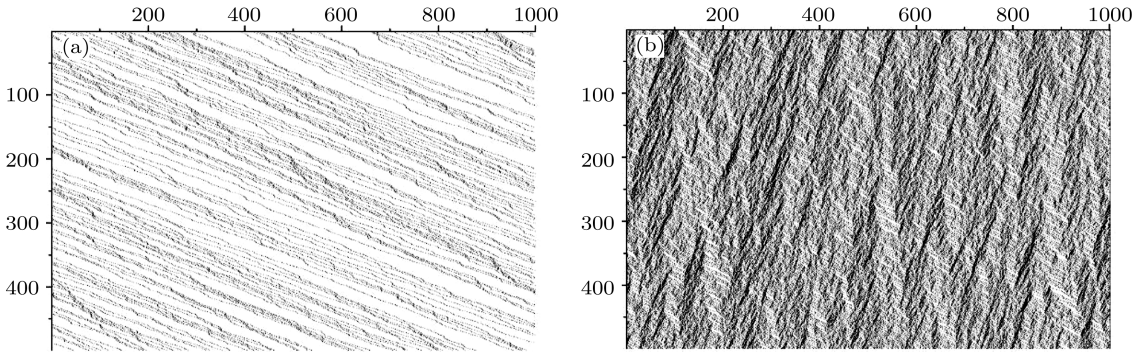


Fig.2. The spatial-temporal diagram of the MWP model, the horizontal direction is space and the vertical direction is time: (a) $k = 0.05$; (b) $k = 0.26$.

In order to identify synchronized flow, we choose stochastically a site and put a virtual loop detector on it. We can obtain data of one minute averaged flow rate J and averaged velocity v by the virtual loop detector. The density is then calculated by $k = J/v$. According to the data, the one minute averaged flow rate-density plane is drawn in Fig.3. One can see that the data are widely scattered, which are consistent with observed features of synchronized flow.

According to Ref.[20], the autocorrelation function and cross-correlation function are shown as follows:

$$a_x(\tau) = \frac{\langle x(t)x(t+\tau)\rangle - \langle x(t)\rangle^2}{\langle x(t)^2\rangle - \langle x(t)\rangle^2}, \tag{6}$$

$$c_{x,y}(\tau) = \frac{\langle x(t)y(t+\tau)\rangle - \langle x(t)\rangle\langle y(t)\rangle}{\sqrt{\langle x(t)^2\rangle - \langle x(t)\rangle^2}\sqrt{\langle y(t)^2\rangle - \langle y(t)\rangle^2}}, \tag{7}$$

where x, y denote the aggregated quantities, $\langle\ \rangle$ denotes the average over the whole series of x. According to the data which is obtained by simulating with the global density of $k = 0.26$ and Eqs.(5), (6), the autocorrelation functions of J, k, v and the cross-correlation functions between J and k are computed.

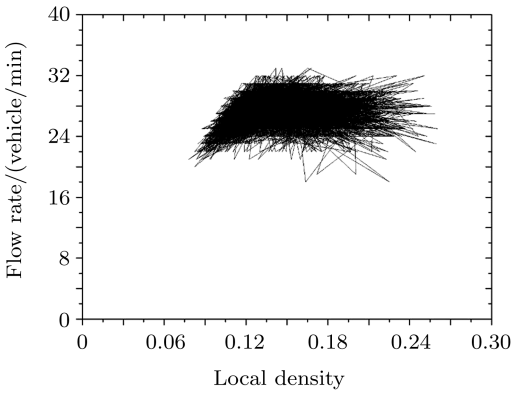


Fig.3. One-minute flux-density diagram with the global density of 0.26.

In Fig.4, it can be seen that the autocorrelation functions of J, k, v are all close to zero, which means that no long-range correlation exists.

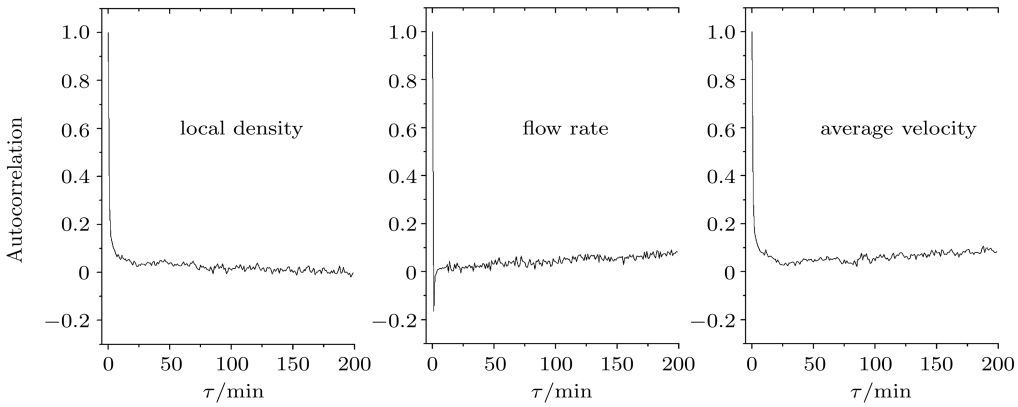


Fig.4. Autocorrelation functions of local flow rate, local density and average velocity with the global density of 0.26.

In Fig.5, one can see that the cross-correlation of local density and local flow rate exists in small time scale and it vanishes in large time scale. These properties are also consistent with observed characteristics of synchronized flow.

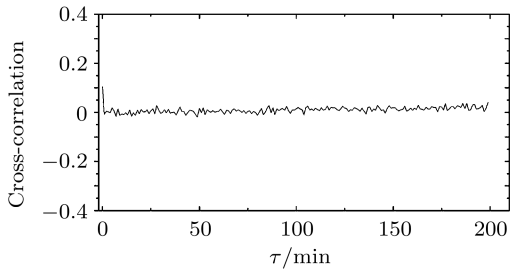


Fig.5. The cross-correlation function between local density and local flow rate with the global density of 0.26.

To sum up, the simulation results of the MWP model are consistent with observed characteristics of synchronized flow.

3.2. On-ramp system

In this subsection, we adopt the MWP model to simulate and discuss the on-ramp system which is shown in Fig.6. The open boundary conditions are applied as follows. Assuming the main road is single lane, the left-most site on the road corresponds to x=1, the position of the left-most (right-most) vehicle is $x_{\rm last}(x_{\rm lead})$, we find that a new vehicle with velocity $v_{\max}$ will be injected to the position $\min(x_{\rm last}-v_{\max}, v_{\max})$ with probability a_1, if $x_{\rm last} > v_{\max}$. At the right boundary, the leading vehicle moves without any hindrance and it will be removed when $x_{\rm lead} > L$, then the following vehicle becomes the new leader. At the on-ramp, a simple setup is adopted, which is similar to the method of Diedrich *et al.*[21] At each time step, every vehicle in the region of the on-ramp $[x_{\rm on}, x_{\rm on}+L_{\rm ramp}]$ is scanned, then the gaps between these vehicles are computed and the longest gap is found out. If this gap is larger than 2, a new vehicle will be injected into the site in the middle of the gap with probability a_2. The velocity of the newly injected vehicle is equal to the velocity of its preceding vehicle. In this paper, $x_{\rm on}=0.8L$ and $L_{\rm ramp}=15$.

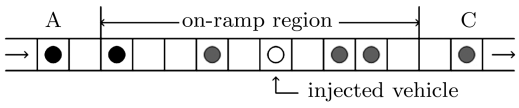


Fig.6. On-ramp system.

In this paper, the congested flow of the on-ramp is defined as that of a vehicle which cannot inject into the main road freely, it means that the injecting rate, i.e. the flow rate of the on-ramp, is smaller than a_2. Figure 7 shows the phase diagram in the (a_1, a_2) space. One can see that three regions are categorized, which is different from previous results.[22,23] In region I, the flows on both the main roads and ramp are free; in region II, it is still a free flow on the main road but becomes congested on the ramp and the flows on both the main roads and the ramp are congested in region III. It is noted that in the phase diagram the region in which the flow on the main road is congested but free on the ramp does not exist. The reason is that when the vehicle on the ramp intents to inject into the main road, it can inject into the main road in conditions of finding the gap which is larger than 2 in the region of the on-ramp. The limitation leads to the case that the vehicle on the ramp hardly injects into the main road, when the density on the main road is very large.

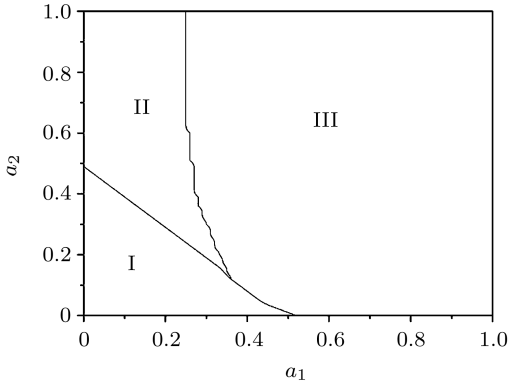


Fig.7. Diagram of traffic patterns.

Firstly, we discuss the flow rates on road A, road C and the ramp, which are denoted by $J_{\rm A}$, $J_{\rm C}$ and $J_{\rm B}$, respectively, as a function of a_1 when a_2 is fixed.

In Fig.8(a), $a_2=0.1$, two ranges of a_1 exist:

i) When $a_1 < a_{11}$, the flows on both the main roads and the ramp are free, the traffic pattern is in region I. The $J_{\rm B}$ remains constant and the $J_{\rm A}$ increases with a_1. As a result, $J_{\rm C}=J_{\rm A}+J_{\rm B}$, $J_{\rm C}$ increases with a_1.

ii) When $a_1 > a_{11}$, the flow on the main road becomes congested and remains constant. The flow rate on the ramp decreases, becomes congested and remains constant. So $J_{\rm A}$, $J_{\rm B}$ and $J_{\rm C}$ are all constant and the traffic pattern is in region III.

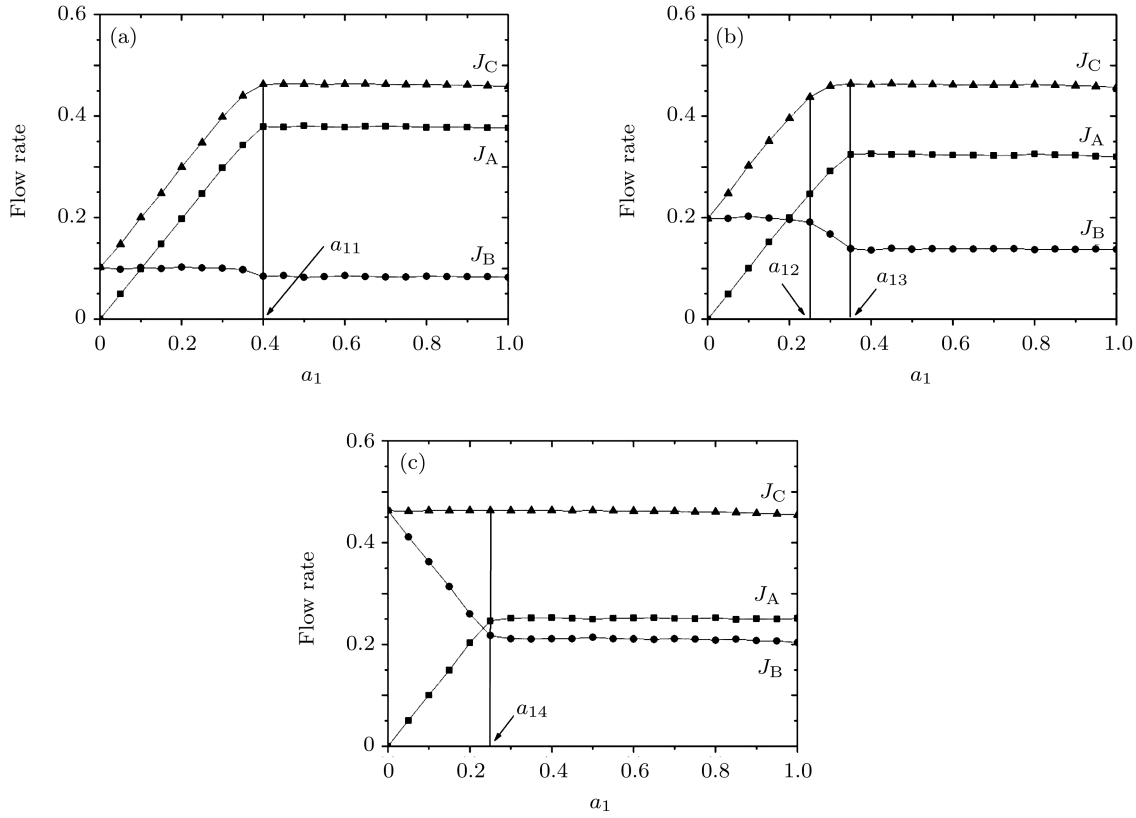


Fig.8. Dependence of the flow rate on a_1 with a_2 fixed: (a) $a_2 = 0.1$; (b) $a_2 = 0.2$; (c) $a_2 = 0.6$.

In Fig.8(b), $a_2 = 0.2$, three ranges of a_1 exist:

1) When $a_1 < a_{12}$, the flows on both the main roads and the ramp are free. The J_B remains constant and the J_A increases with a_1. As a result, the J_C increases with a_1 and the traffic pattern is in region I.

2) When $a_{12} < a_1 < a_{13}$, it is still a free flow on the main road but becomes congested on the ramp and the traffic pattern is in region II. The J_B decreases with a_1 while the J_A increases with a_1. The $J_C = J_A + J_B$ and J_C increases with a_1.

3) When $a_1 > a_{13}$, the flows on both the main roads and the ramp are congested and remain constant and the traffic pattern is in region III. But the J_B is smaller than that in region I. As a result, the J_C turns into the constant.

In Fig.8(c), $a_2 = 0.6$, there are still two ranges of a_1:

a) When $a_1 < a_{14}$, it is still free flow on the main road and the J_A increases with a_1, but becomes congested on the ramp and the J_B decreases with a_1. The $J_C = J_A + J_B$ retain constant and the traffic pattern is in region II.

b) When $a_1 > a_{14}$, the flows on both the main roads and the ramp are congested and J_A, J_B and J_C retain constant. The traffic pattern is in region III.

Secondly, we fix the value of a_1 and study the dependence of the three flow rates on a_2. In Fig.9, the typical curves are given.

In Fig.9(a), $a_1 = 0.2$, a_2 is classified into two ranges:

i) When $a_2 < a_{21}$, the flows on both the main roads and the ramp are free. The J_A remains constant, and the J_B increases with a_2. As a result, the J_C increases with a_2. The traffic pattern is in region I.

ii) When $a_2 > a_{21}$, it is still free flow on the main road and remains constant, but becomes congested on the ramp and also remains constant. As a result, the J_C remains constant and the traffic pattern is in region II.

In Fig.9(b), $a_1 = 0.3$, a_2 is classified into three ranges:

i) When $a_2 < a_{22}$, the flows on both the main roads and the ramp are free. The J_A remains constant and the J_B increases with a_2. As a result, $J_C = J_A + J_B$, the J_C increases with a_2. The traffic pattern is in region I.

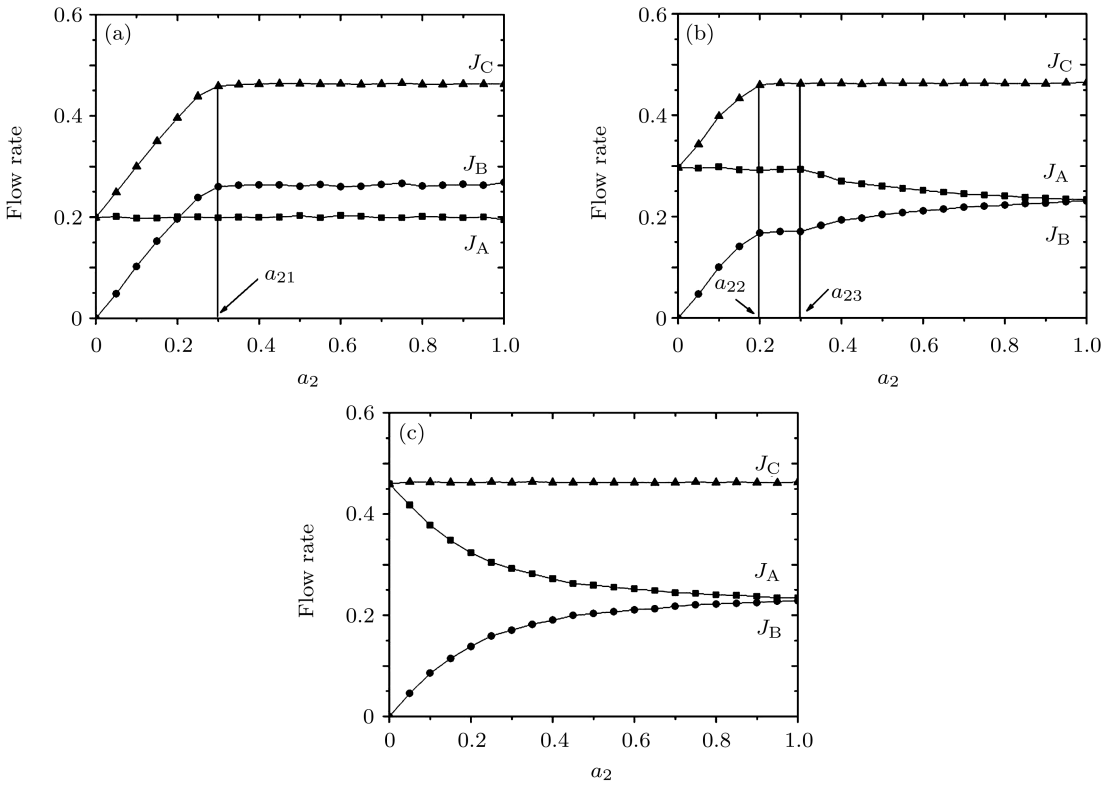


Fig.9. Dependence of the flow rate on a_2 with a_1 fixed: (a) $a_1 = 0.2$; (b) $a_1 = 0.3$, (c) $a_1 = 0.6$.

ii) When $a_{22} < a_2 < a_{23}$, it is still free flow on the main road but becomes congested on the ramp. The J_A remains still constant and the J_B also remains constant. As a result, $J_C = J_A + J_B$ remains constant, the traffic pattern is in region II.

iii) When $a_2 > a_{23}$, the flows on both the main roads and the ramp are congested. The J_A decreases with a_2, the J_B increases with a_2, and $J_A + J_B$ is invariable. As a result, the J_C remains constant and the traffic pattern is in region III.

In Fig.9(c), $a_1 = 0.6$, the flows on both the main roads and the ramp are congested. The J_A decreases with a_2, the J_B increases with a_2. The difference between J_A and J_B becomes smaller and smaller with a_2 and almost vanishes when $a_2 = 1$. It means that flow rates on both the main roads and ramp are almost equal, when the road is in a saturated state, which is consistent with our observed result in real traffic.[24]

Finally, through the flow rate analysis above, we can conclude that when the entering probability of the main road is large enough ($a_1 > 0.5$), the phase diagram is categorized into three regions. And the region in which flow on the main road is congested but free on the ramp does not exist, though a_2 is very small.

4. Conclusion

This paper improves the WP model by considering the velocity effects at the last time step. In the modified model, the vehicle deceleration is restricted in an advisable range, which describes the complex traffic behaviors more appropriately.

The numerical results show that the MWP model can obtain a higher flow rate and reproduce synchronized flow. Then we use the MWP model to simulate a road system with a virtual on-ramp. The phase diagram shows that there exist three phases. Due to the unique rules of our model, the phase for which the traffic flow is congested flow on the main lane while free flow on the on-ramp does not exist. The relations of flow rate and entering probability, including on-ramp flow rate, upstream flow rate on the main lane, and

downstream flow rate on the main lane, are discussed.

However, in this paper we have applied a simplified treatment with the on-ramp, which is different from a real one. Therefore our work is going to be continued by modeling real on-ramp systems based on the MWP model, and setting up reasonable rules to represent drivers' complex behaviors while entering the main lane from the on-ramp.

References

[1] Chowdhury D, Santen L and Schadschneider A 2000 *Phys. Rep.* **329** 199

[2] Helbing D 2001 *Rev. Mod. Phys.* **73** 1067

[3] Maerivoet S and De Moor B 2005 *Phys. Rep.* **419** 1

[4] Jia B, Gao Z Y, Li K P and Li X G 2007 *Models and Simulations of Traffic System Based on the Theory of Cellular Automaton* (Beijing: Science Press) p68

[5] Nagel K and Schreckenberg M 1992 *J. Phys. I* (France) **2** 2221

[6] Xue Y, Dong L Y and Dai S Q 2001 *Acta Phys. Sin.* **50** 445 (in Chinese)

[7] Tan H L, Liu M R and Kong L J 2002 *Acta Phys. Sin.* **51** 2713 (in Chinese)

[8] Lei L, Xue Y and Dai S Q 2003 *Acta Phys. Sin.* **52** 2121 (in Chinese)

[9] Bai K Z, Tan H L, Liu M R and Kong L J 2003 *Acta Phys. Sin.* **52** 2421 (in Chinese)

[10] Huang B H, Kong L J and Liu M R 2001 *Acta Phys. Sin.* **50** 30 (in Chinese)

[11] Hua W and Lin B L 2005 *Acta Phys. Sin.* **54** 2595 (in Chinese)

[12] Mu Y B and Zhong C W 2005 *Acta Phys. Sin.* **54** 5597 (in Chinese)

[13] Tian L J, Liu T L and Huang H J 2008 *Acta Phys. Sin.* **57** 2122 (in Chinese)

[14] Fukui M and Ishibashi Y 1996 *J. Phys. Soc. Jpn.* **65** 1868

[15] Li X B, Wu Q S and Jiang R 2001 *Phys. Rev.* E **64** 066128

[16] Masahiro K, Katsuhiro N and Tetsuji T 2005 *Phys. Rev.* E **72** 035102

[17] Bando M, Hasebe K, Nakayama A, Shibata A and Sugiyama Y 1995 *Phys. Rev.* E **51** 1035

[18] Bando M, Hasebe K, Nakanishi K, Nakayama A, Shibata A and Sugiyama Y 1995 *J. Phys.* I **5** 1389

[19] Li X L, Kuang H, Song T, Dai S Q and Li Z P 2008 *Chin. Phys.* B **17** 2366

[20] Gao K, Jiang R, Hu S X, Wang B H and Wu Q S 2007 *Phys. Rev.* E **76** 026105

[21] Diedrich G, Santen L, Schadschneider A and Zittartz J 2000 *Int. J. Mod. Phys.* C **11** 335

[22] Jiang R and Wu Q S 2002 *Phys. Rev.* E **66** 036104

[23] Jiang R, Jia B and Wu Q S 2003 *J. Phys.* A **36** 11713

[24] Jia B, Li X G, Guo H W and Xie D F 2008 *Technical Report* (Institute of System Sciences, School of Traffic and Transportation, Beijing Jiaotong University)